AJNR

Diffusion-weighted MR Imaging of Intracerebral Masses: Comparison with Conventional MR Imaging and Histologic Findings

Tadeusz W. Stadnik, Cristo Chaskis, Alex Michotte, Wael M. Shabana, Katrijn van Rompaey, Robert Luypaert, Lubos Budinsky, Vladimir Jellus and Michel Osteaux

AJNR Am J Neuroradiol 2001, 22 (5) 969-976
http://www.ajnr.org/content/22/5/969

AJNR Am J Neuroradiol 22:969–976, May 2001

Diffusion-weighted MR Imaging of Intracerebral Masses: Comparison with Conventional MR Imaging and Histologic Findings

Tadeusz W. Stadnik, Cristo Chaskis, Alex Michotte, Wael M. Shabana, Katrijn van Rompaey, Robert Luypaert, Lubos Budinsky, Vladimir Jellus, and Michel Osteaux

BACKGROUND AND PURPOSE: **The purposes of this study were to find the role of diffusion-weighted MR imaging in characterizing intracerebral masses and to find a correlation, if any, between the different parameters of diffusion-weighted imaging and histologic analysis of tumors. The usefulness of diffusion-weighted imaging and apparent diffusion coefficient (ADC) maps in tumor delineation was evaluated. Contrast with white matter and ADC values for tumor components with available histology were also evaluated.**

METHODS: **Twenty patients with clinical and routine MR imaging/CT evidence of intracerebral neoplasm were examined with routine MR imaging and echo-planar diffusion-weighted imaging. The routine MR imaging included at least the axial T2-weighted fast spin-echo and axial T1-weighted spin-echo sequences before and after contrast enhancement. The diffusion-weighted imaging included an echo-planar spin-echo sequence with three b values (0, 300, and 1200 s/mm), sensitizing gradient in the z direction, and calculated ADC maps. The visual comparison of routine MR images with diffusion-weighted images for tumor delineation was performed as was the statistical analysis of quantitative diffusion-weighted imaging parameters with histologic evaluation.**

RESULTS: **For tumors, the diffusion-weighted images and ADC maps of gliomas were less useful than the T2-weighted spin-echo and contrast-enhanced T1-weighted spin-echo images in definition of tumor boundaries. Additionally, in six cases of gliomas, neither T2-wighted spin-echo nor diffusion-weighted images were able to show a boundary between tumor and edema, which was present on contrast-enhanced T1-weighted and/or perfusion echo-planar images. The ADC values of solid gliomas, metastases, and meningioma were in the same range. In two cases of lymphomas, there was a good contrast with white matter, with strongly reduced ADC values. For infection, the highest contrast on diffusion-weighted images and lowest ADC values were observed in association with inflammatory granuloma and abscess.**

CONCLUSION: **Contrary to the findings of previous studies, we found no clear advantage of diffusion-weighted echo-planar imaging in the evaluation of tumor extension. The contrast between gliomas, metastases, meningioma, and white matter was generally lower on diffusion-weighted images and ADC maps compared with conventional MR imaging. Unlike gliomas, the two cases of lymphomas showed hyperintense signal on diffusion-weighted images whereas the case of cerebral abscess showed the highest contrast on diffusion-weighted images with very low ADC values. Further study is required to find out whether this may be useful in the differentiation of gliomas and metastasis from lymphoma and abscess.**

The high sensitivity and specificity of echo-planar diffusion-weighted imaging in the diagnosis of acute cerebral infarction is widely accepted (1). The reduced diffusion typical of acute stroke is thought to be related to the cytotoxic edema and shrinking of the extracellular space (2, 3). We can hypothesize that diffusion-weighted imaging may enable us to differentiate various tumor components and to distinguish tumoral invasion from normal tissue or edema. This distinction, if possible, would be very important for planning surgical resection, biopsies, and radiation therapy.

Diffusion-weighted MR imaging has been used by some to evaluate intra-axial tumors. Brunberg et al (4) reported that the apparent diffusion coefficient (ADC) values and index of diffusion an-

Received September 4, 1998; accepted after revision November 15, 2000.

From the Departments of Radiology and Medical Imaging (T.W.S., W.M.S., R.L., M.O.). Neurosurgery (C.C., K.V.R.), and Neurology and Pathology (A.M.), University Hospital V.U.B., Brussels, Belgium; and the Laboratory of Tomographic Methods (L.B., V.J.), Institute of Measurement Science, Slovak Academy of Sciences, Bratislava, Slovakia.

Address reprint requests to T. Stadnik, Department of Radiology and Medical Imaging, University Hospital V.U.B., Laarbeeklaan 101, 1090 Brussels, Belgium.

TABLE 1: Summary of histologic diagnoses

Histologic Diagnosis	Number of Cases
Gliobastoma	6
Astrocytoma II or III	4
Pilocytic astrocytoma	1
Lymphoma	2
Meningioma	2
Metastases	2
Infarct	1
Granulomas	1
Abscess	1
Total	20

isotropy (index of diffusion anisotropy = ADC maximum − ADC minimum/ADC mean) distinguished normal white matter areas from necrosis and cyst formation, edema, and solid enhancing tumor. Tien et al (5) found that areas of enhancing tumor were relatively hyperintense on diffusion-weighted images and that it was possible to distinguish areas of predominantly unenhanced tumor from areas of predominantly peritumoral edema when the abnormality was located in white matter and aligned in the direction of the diffusion-weighted gradient. Krabbe et al (6) reported that ADC values in contrast-enhancing areas within cerebral metastases were statistically significantly higher than the ADC values in contrast-enhancing areas in cases of high grade gliomas.

The purposes of our study were as follows: 1) to compare the capability of conventional MR imaging and diffusion-weighted imaging to delineate components of brain tumor; 2) to evaluate diffusion-weighted images and ADC maps of contrast-enhancing components of tumors; 3) to calculate contrast and ADC values for tumor components confirmed by histology; 4) to find a correlation, if any, between different parameters of diffusion-weighted imaging and histologic analysis of tumors.

Methods

Between August 1996 and February 1998, 20 patients with clinical and routine MR imaging/CT evidence of cerebral masses were examined with routine MR imaging and echo-planar diffusion-weighted imaging on a Siemens Vision 1.5-T imager (Siemens, Erlangen, Germany) (Table 1). The routine MR imaging included an axial T2-weighted fast spin-echo sequence (6000/90 [TR/TE]; signals acquired, one or two; section thickness, 6 mm; echo train length, 23; matrix, 192 × 256 or 230 × 512; field of view, 184 × 205 or 230 × 230 mm) and an axial T1-weighted spin-echo sequence (600/14; signals acquired, two or three; section thickness, 6 mm; matrix, 220 × 256; field of view, 230 × 230 mm) before and after injection of contrast material.

Between August 1996 and February 1997, the diffusion-weighted imaging included an axial echo-planar spin-echo sequence (800/123; signals acquired, 10; section thickness, 6 mm; matrix, 128 × 200; field of view, 280 × 280 mm; three b values of 0, 300, and 1200 s/mm^2; sensitising gradient in the z direction in all cases and occasionally in the x and y directions). δ (duration) and G (amplitude) of the pulsed gradients were 26 ms and 0, 11, and 22 mT/m, respectively. Δ (distance between the leading edges of the two pulsed gradients) was 59.7 ms.

Since February 1997, the previous sequence was implemented with tensor, Eigen values, and anisotropy calculations (800/123; signals acquired, five; section thickness, 6 mm; matrix, 128 × 200; field of view, 280 × 280 mm; three b values of 0, 300, and 1200 s/mm^2; sensitising gradients in the z, x, y, zx, zy, and xy directions).

Comparison of Mass Delineation between Conventional MR Imaging and Diffusion-weighted Imaging

Neither contrast-enhanced images nor T2-weighted images can reliably define tumor boundaries. Therefore, the observers were asked to report only if apparent tumor boundaries available on contrast-enhanced T1-weighted spin-echo and fast T2-weighted spin-echo images were better, equally, or less well delineated on diffusion-weighted images and ADC maps. All images were interpreted by two experienced neuroradiologists (T.W.S., W.M.S.). When disagreement arose, a third neuroradiologist (M.O.) adjudicated.

Previous reports (5) suggest that areas of contrast-enhancing tumor were markedly hyperintense on diffusion-weighted images. Therefore, the observers were asked also to report whether enhancing tumor areas were hyper-, iso-, or hypointense on diffusion-weighted images and ADC maps with respect to the underlying white matter.

It is well known that differentiation between tumor invasion and edema is frequently impossible using conventional MR imaging. In such cases (presence of peritumoral or diffuse hyperintensity on T2-weighted spin-echo images without contrast material uptake on T1-weighted spin-echo images) the observers were also asked to report presence or not on diffusion-weighted images and ADC maps of signal intensity variations that may suggest the presence of tumoral invasion (ie, areas with signal intensity similar to that of the histologically proven tumoral components).

Comparison of Quantitative Diffusion-weighted Imaging Parameters with Histologic Evaluation

For nine patients, the biopsy was performed using a stereotactic frame. For 11 patients, the neurosurgeon was asked to perform the biopsies in predefined areas of tumor. The histologic analysis of the biopsies included the evaluation of cellularity, vascularity, endothelial abnormalities, malignity using 4-digit notification (eg, 0 = no, 1 = low, 2 = medium, 3 = high), and volume of extracellular space using 3-digit notification (eg, 1 = small, 2 = medium, 3 = large).

The following diffusion-weighted imaging parameters were calculated for stereotactic biopsy targets or for surgical biopsy areas. Contrast between target/white matter on contrast-enhanced T1-weighted spin-echo and diffusion-weighted images was defined as (signal intensity of target − signal intensity of white matter)/signal intensity of noise. Signal intensity of noise is signal intensity of the region of interest measured outside the skull of the patient. Contrast between target/white matter on ADC maps was defined as (signal intensity of target − signal intensity of white matter)/((signal intensity of target + signal intensity of white matter)/2). ADC values for target and white matter were obtained in the z, x, and y directions and, when available, ADC values of trace and Eigen values were also obtained. ADC values were expressed in 10^{-9} m^2/s. The regions of interest for the calculation of ADC values for white matter were chosen in the areas of low anisotropy (eg, in frontal or occipital lobes).

The lattice index maps are also available for eight patients (four glioblastomas, one astrocytoma, one granuloma, one meningioma, and one abscess). The lattice index was calculated using a modification of the technique described by Pierpaoli and Basser (7) and provides a scalar measure for the degree

TABLE 2: Comparison of fast T2-weighted spin-echo and contrast-enhanced T1-weighted spin-echo with diffusion-weighted echo-planar imaging and ADC maps in delineation of cerebral tumor boundaries (n = 17)*

Histologic Diagnosis (number of cases)	T2SE = DWI	T2SE = ADC Maps	T1SE + Gd = DWI	T1SE + Gd = ADC Map
Gliobastoma (6)	0	2	0	0
Astrocytoma (4)	0	2	0	2
Pilocytic astrocytoma (1)	1	1	1	1
Lymphoma (2)	2	0	1	0
Meningioma (2)	0	0	0	0
Metastases (2)	1	1	0	0

* Only the cases judged equivalent are reported. In the remaining cases the T2-weighted spin-echo or contrast-enhanced T1-weighted spin-echo/diffusion-weighted imaging were judged superior to diffusion-weighted imaging and ADC maps.

Note.—T2SE indicates T2-weighted spin-echo; DWI, diffusion-weighted imaging; T1-weighted contrast-enhanced spin-echo.

of intervoxel anisotropy coherence (ie, the similarity in the anisotropy characteristics of adjacent voxels).

Pearson statistical analysis was used to correlate the histologic evaluation with the imaging parameters. $P < .05$ was considered to indicate a statistically significant correlation, and $P = .05$ to .10 was considered to be marginally significant.

Results

Twenty patients (six glioblastomas, four astrocytomas, one pilocytic astrocytoma, two lymphomas, two metastasis, two metastases, two meninigiomas, one infarct, one granuloma, and one abscess) were available for evaluation (Table 1). A comparison of mass delineation between conventional MR imaging and diffusion-weighted imaging is shown in Table 2.

Glial Tumors

In all cases of glioblastoma (six cases) and astrocytomas (four cases) the diffusion-weighted images were judged to be inferior to the T2-weighted spin-echo and contrast-enhanced T1-weighted spin-echo images in mass delineation. The solid components were frequently heterogeneous and difficult to differentiate from white matter (Fig 1).

The calculated ADC maps did a little better than did the diffusion-weighted images. The delineation was judged to be equivalent to that on the T2-weighted spin-echo and/or contrast-enhanced T1-weighted spin-echo images in two of six cases of gliobastomas and in two of four cases of astrocytoma. For the remaining cases of gliomas, the diffusion-weighted images and ADC maps were judged to be inferior to the T2-weighted spin-echo and contrast-enhanced T1-weighted spin-echo images (Fig 2).

Lymphomas

The delineation of lymphomas on diffusion-weighted images was equivalent to that on the T2-weighted spin-echo and/or contrast-enhanced T1-weighted spin-echo imaging in both cases (Fig 3) but was inferior on ADC maps.

Meningioma

The delineation of meningioma on diffusion-weighted images and ADC maps was inferior to that on T2-weighted spin-echo and contrast-enhanced T1-weighted spin-echo images.

Metastases

The delineation of metastases on the diffusion-weighted images was inferior to that on the contrast-enhanced T1-weighted spin-echo images in two cases and equivalent to that on the T2-weighted MR images in one case.

Evaluation of Enhancing Tumor Areas with Diffusion-weighted Images and ADC Maps

Glial Tumors.—The enhancing components of glioblastomas (six cases) on diffusion-weighted images generally showed a mixture of hyper- and isointensities with respect to white matter (Fig 2). The calculated contrast values on the diffusion-weighted images were in the range of 0.3 to 4.6 (mean, 1.8). The calculated ADC values were in the range of 0.78 to 1.79 (mean, 1.14).

Lymphomas.—In two cases of lymphomas, the enhancing components were hyperintense on diffusion-weighted images. The contrast with white matter was as high as 9.4 (Fig 3). The corresponding ADC values were as low as 0.58 and 0.55.

Meningioma.—Meningioma was nearly isointense with white matter on the diffusion-weighted images (Table 3), and the ADC values were only slightly superior to those of white matter (Table 4).

Metastases.—Two cases of metastases were isointense to slightly hyperintense to white matter (Table 3, contrast 1 and 3). The calculated ADC values were 0.82 and 1.24.

Diffusion-weighted Images and ADC Maps in Peritumoral Areas

In case of peritumoral hyperintensity on fast T2-weighted spin-echo images without evidence of tumor invasion on contrast-enhanced T1-weighted images, the diffusion-weighted images and ADC maps did not show a consistent signal intensity variation, which could suggest the presence of tumoral invasion and advocate the stereotactic confirmation.

Quantitative Diffusion-weighted Imaging Parameters and Histologic Evaluation

Diffusion-weighted Imaging.—For gliomas, the calculated tumor:white matter contrast values on

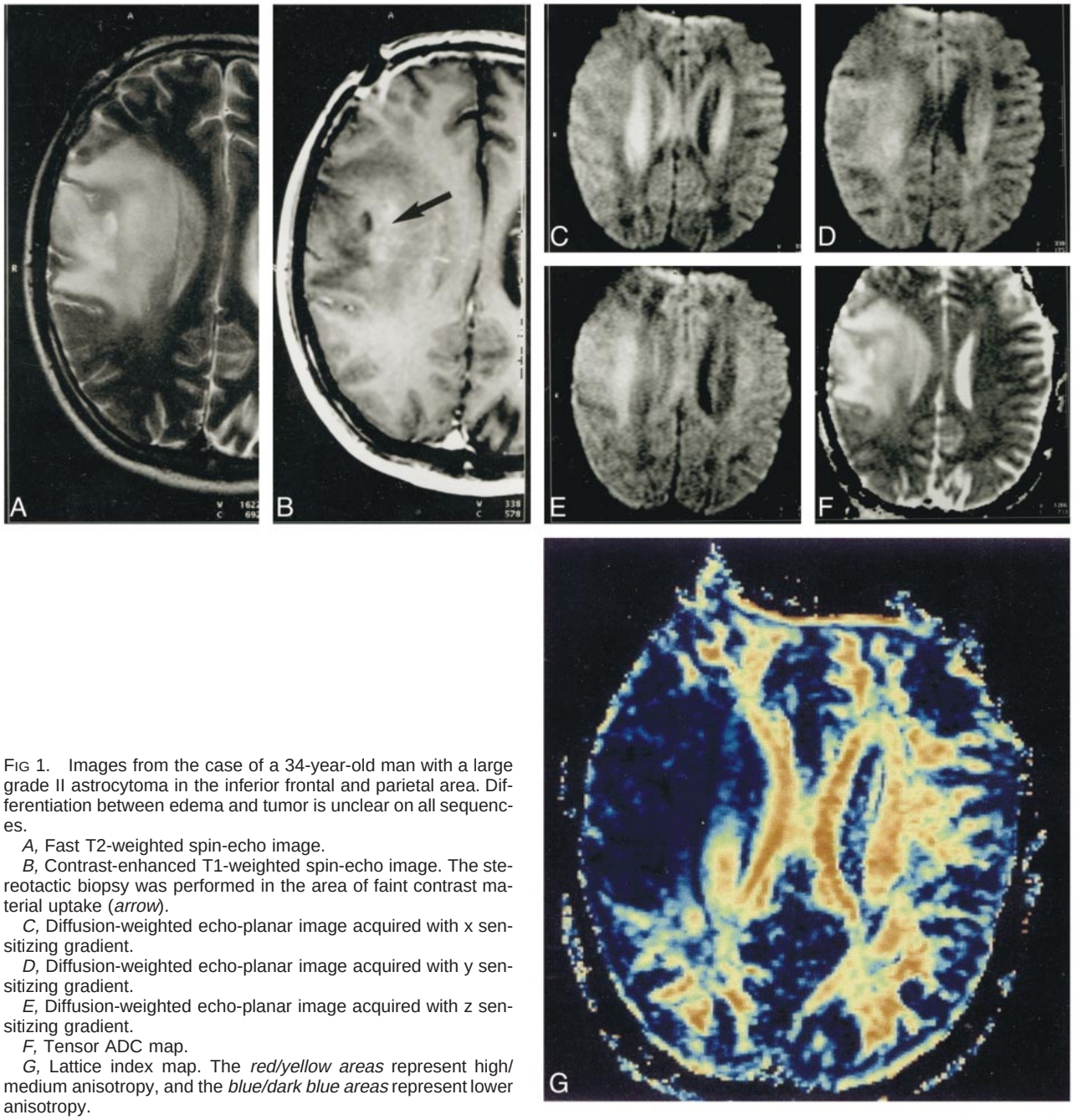

FIG 1. Images from the case of a 34-year-old man with a large grade II astrocytoma in the inferior frontal and parietal area. Differentiation between edema and tumor is unclear on all sequences.

A, Fast T2-weighted spin-echo image.

B, Contrast-enhanced T1-weighted spin-echo image. The stereotactic biopsy was performed in the area of faint contrast material uptake (*arrow*).

C, Diffusion-weighted echo-planar image acquired with x sensitizing gradient.

D, Diffusion-weighted echo-planar image acquired with y sensitizing gradient.

E, Diffusion-weighted echo-planar image acquired with z sensitizing gradient.

F, Tensor ADC map.

G, Lattice index map. The *red/yellow areas* represent high/medium anisotropy, and the *blue/dark blue areas* represent lower anisotropy.

diffusion-weighted images obtained in the z direction were generally low (range, 0.3–4.6; mean, 2.2) (Table 3). These contrast values were also low in cases of meningioma and metastases. However, the two cases of intracerebral lymphomas were strongly hyperintense on diffusion-weighted images (contrast with white matter as high as 9.4) (Fig 3). The highest contrast (24) was observed in one case of cerebral abscess. This finding was helpful in the differential diagnosis with necrotic glioblastoma (Table 3) (Fig 4).

ADC Values in the z Direction.—The ADC values ($\times 10^{-9}$ m^2/s) for solid components of gliomas measured in the z direction were in the range of 0.71 to 1.48 (mean, 1.14). These values are superior to the ADC values of white matter (range, 0.55−0.78; mean, 0.63). The ADC values for meningioma and metastases were in the range of the ADC values of gliomas (Table 4.). However, the ADC values of lymphomas were as low as 0.58 and 0.55, respectively. The lowest ADC value was observed in a case of cerebral abscess (0.29) and granulomas (0.39).

Statistical Analysis of Solid Tumor Components.—There was a high correlation ($P < .01$) between the contrast values measured on diffusion-weighted images and the histologic evaluation of the volume of extracellular space. The ADC values were also strongly correlated with the extracellular space ($P = .04$). On the other hand, there was no

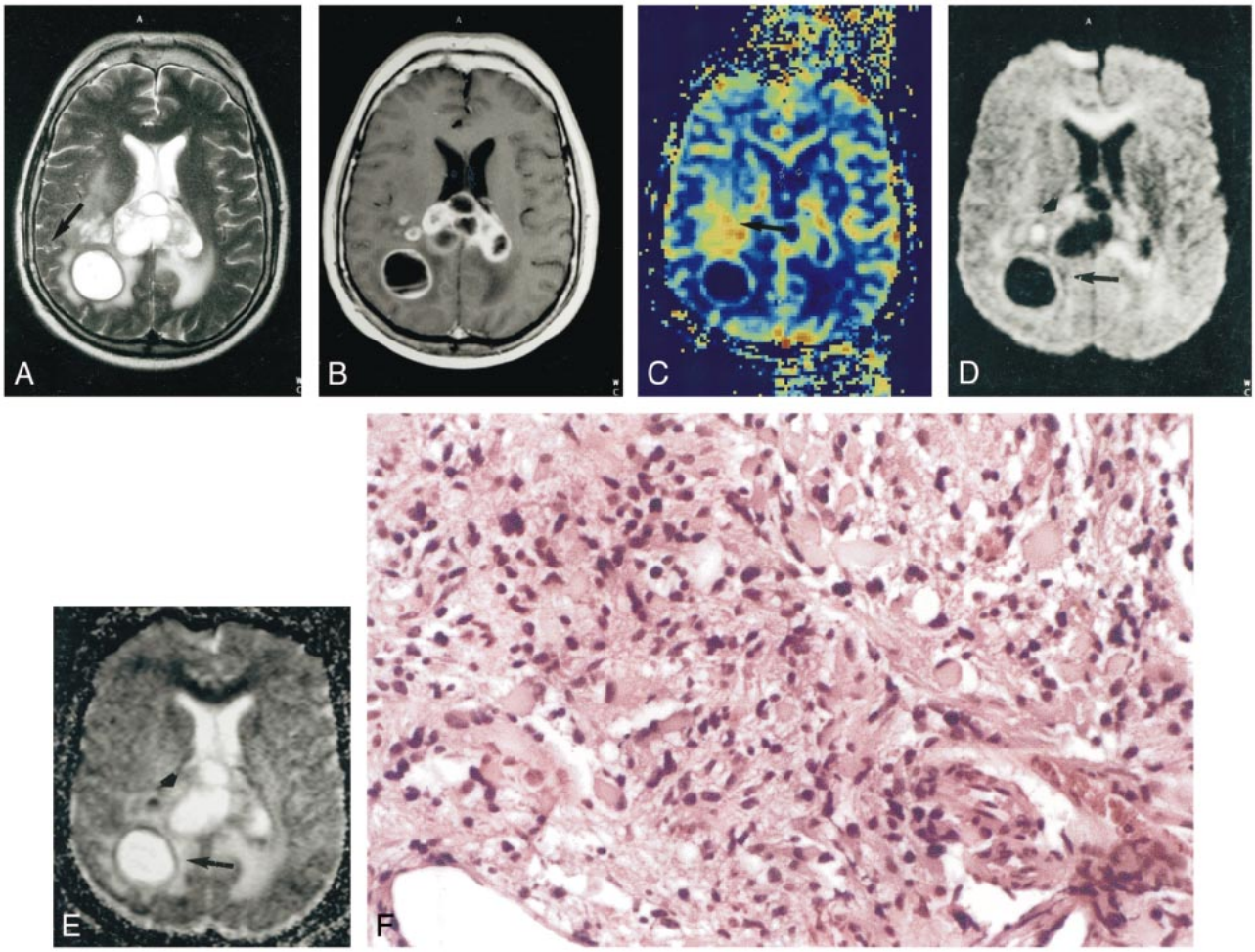

FIG 2. Images from the case of a 52-year-old man with a large glioblastoma.

A, Invasion of corpus callosum and of occipitotemporal white matter is recognized on fast T2-weighted spin-echo image.

B, Invasion of corpus callosum and of occipitotemporal white matter is recognized on contrast-enhanced T1-weighted spin-echo image.

C, Invasion of subinsular white matter is clearly recognized only on the perfusion-weighted echo-planar image (*arrow*).

D, On the diffusion-weighted image, only cystic components of tumor are clearly shown. There is no clear difference between contrast-enhancing tumor (*arrowhead*) and edema (*arrow*).

E, On the ADC map, only cystic components of tumor are clearly shown. There is no clear difference between contrast-enhancing tumor (*arrowhead*) and edema (*arrow*).

F, Histologic examination (hematoxylin and eosin; original magnification, ×250) shows a medium sized extracellular space and moderate cellularity.

significant correlation between the number of cells and contrast enhancement on diffusion-weighted images or ADC maps ($P = .16$ and .23, respectively). There was no correlation between the degree of malignancy (for intra-axial tumors, including metastases and lymphomas) and the contrast on diffusion-weighted images versus ADC maps ($P = .6$ and .9, respectively).

The ADC values calculated in six directions (as well as trace and Eigen values) were available in six cases (four glioblastomas, one astrocytoma, and one meningioma). The ADC values for solid tumor components (range, 0.84–2.4; mean, 1.11) and for white matter (range, 0.69–0.84; mean, 0.71) provided by trace were similar to the values measured in the z directions. The Eigen values sorted for white matter also showed lower values than the Eigen values sorted for gliomas (range, 0.3–1.12 and 0.88–1.5, respectively). Similarly, on lattice index maps, a striking contrast was observed between high anisotropy areas of white matter and tumor areas. However, this contrast was much lower between low anisotropy white matter, gray matter, and tumor areas (Fig 1E).

Discussion

Diffusion-weighted imaging has been most conclusive in the differentiation of epidermoid from arachnoid cysts (8, 9). The diffusion of water in white matter is restricted (10, 11), and diffusion-weighted imaging may be potentially useful in differentiation between solid tumor and edema as well as in tissue characterization.

Brunberg et al (4) used a motion-insensitive spin-echo sequence that uses standard MR imaging hardware with diffusion characterized in a single column of interest in 40 patients with cerebral gli-

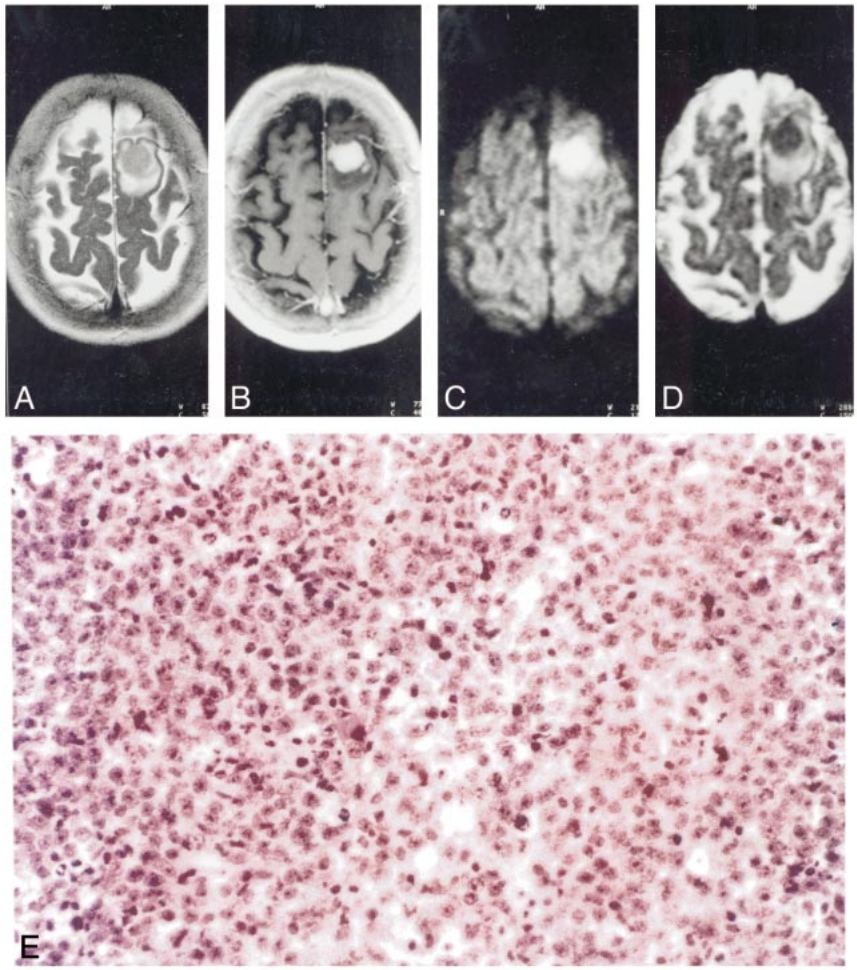

FIG 3. Images from the case of a 72-year-old woman with a cerebral lymphoma. *A,* Fast T2-weighted spin-echo image shows lesion to be moderately hyperintense. *B,* T1-weighted spin-echo image shows strong enhancement of lesion after the administration of contrast material. *C,* Diffusion-weighted image shows the lymphoma also to be hyperintense. *D,* ADC values are in the range of 0.55 to 0.6, similar to the values described in association with acute infarction. *E,* Histologic examination (hematoxylin and eosin; original magnification, ×250) shows high cellularity and small extracellular space, which was significantly associated with reduced ADC values.

TABLE 3: Tumor/white matter contrast values on diffusion-weighted images acquired in "z" direction for solid components

Histologic Diagnosis	Number of Cases	Contrast on Diffusion-weighted Images	
		Range	Mean
Gliomas	11	0.3–4.6	2.2
Lymphoma	2	7.1–9.4	8.3
Meningioma	2	0.5–1.5	1.0
Abscess	1	24	24.0
Infarct	1	9.5	9.5
Granuloma	1	3.6	3.6
Metastases	2	1–3	2.0

TABLE 4: ADC's values for solid tumor components and for white matter acquired in "z" direction

Histologic Diagnosis	Number of Cases	ADC's Tumor		ADC's White Matter	
		Range	Mean	Range	Mean
Gliomas	11	0.71–1.74	1.14	0.55–0.75	0.66
Lymphoma	2	0.55–0.6	0.58	0.55–0.58	0.56
Meningioma	2	0.75–0.95	0.85	0.75–0.78	0.765
Abscess	1	. . .	0.29	. . .	0.56
Infarct	1	. . .	0.55	. . .	0.62
Granuloma	1	. . .	0.39	. . .	0.59
Metastasis	2	0.82–1.24	1.03	0.68–0.69	0.685

omas. ADC values were determined in only a columnar region of interest of $0.8 \times 0.8 \times 20$ cm. The authors found a mean ADC value in enhancing tumor of 1.31×10^{-9} m^2/s (1.14 in our study), in unenhanced solid tumor of 1.43, and in normal white matter of 0.83 (0.63 in our study). Considering the differences in data acquisitions, these results are in agreement. The mean values for ADC and index of diffusion anisotropy were significantly different between tumor and normal white matter. However, there was no difference between ADC values derived from regions of edema and those derived from regions of enhancing or unenhanced tumor. These results are in agreement with our evaluation of tumor delineation on ADC maps (for 11 gliomas, only six ADC maps were judged equivalent to T2-weighted spin-echo and/or enhanced T1-weighted spin-echo images, with the remaining being less useful). This poor delineation between gliomas, edema, and white matter on diffusion-weighted imaging may be easily explained by the conjoined effect of T2 and ADC values. The different ADC values of white matter, gliomas, and edema are counter-compensated by T2 values.

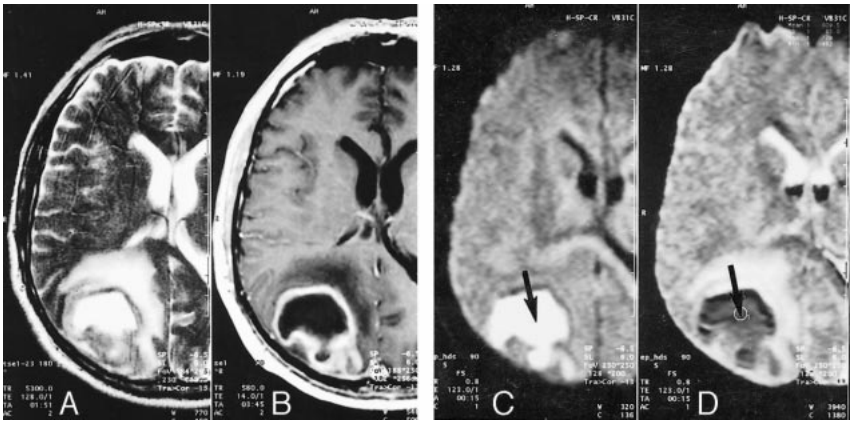

FIG 4. Images from the case of a 70-year-old man with a streptococcus abscess, recent history of acute dizziness, and focal seizures.

A, T2-weighted spin-echo image is consistent with the diagnosis of glioblastoma or necrotic metastasis.

B, Contrast-enhanced T1-weighted spin-echo image is consistent with the diagnosis of glioblastoma or necrotic metastasis.

C, On the diffusion-weighted echo-planar image, however, the ''necrotic'' area shows high signal intensity (*arrow*).

D, On the ADC map, very low ADC values (0.29 e^{-3} mm^2/s) are found (*arrow*). Such behavior was never present in the necrotic parts of gliomas (compare with Fig. 3D and E) or metastases and may be highly specific for abscess formation.

The ADC maps are independent of T2 effects, but the differences between edema and gliomas are small, which explains poor results of ADC maps in differentiation between tumor and edema. Only the differentiation between edema and white matter is satisfactory, but this is also available on T2-weighted sequences.

Brunberg et al (4) found a significant difference in mean diffusion anisotropy between the region of edema and tumor. In our study, the lattice index maps provided high contrast between tumor and high anisotropy white matter. However, the contrast between tumor and edema was much lower.

In another study of 10 patients with high grade gliomas, Tien et al (5) used echo-planar diffusion-weighted images, measuring ADC along the cephalocaudal axis in a single coronal section. They found a mean ADC value in enhancing tumor of 1.1×10^{-9} m/s (1.14 in our study), in unenhanced solid tumor of 1.16, and in white matter between 0.5 and 1.5 (depending on the direction of white matter fibers). Our findings in patients with high grade gliomas are in good agreement. Tien et al also found that unenhanced tumor and vasogenic edema involving corticospinal tracts could have similar ADC values, but the diffusion-weighted echo-planar imaging allow the differentiation between edema and tumor when the abnormality was located in white matter aligned in the direction of the diffusion-weighted gradient. The differentiation between edema and tumor invasion of the white matter tract was based on different signal intensity suppression on diffusion-weighted images, whereas the ADC measurements showed no variations. Furthermore, the histologic confirmation for differentiation of unenhanced tumor/edema was not provided, and this finding remains speculative.

In our study, the signal intensity of gliomas was frequently heterogeneous (iso- or hyperintense with respect to white matter) and the exact delineation was generally judged to be less convincing than on T2-weighted spin-echo and contrast-enhanced T1-weighted spin-echo images.

Recently, Krabbe et al (6) evaluated the cases of 28 patients with intracranial masses (12 high grade and three low grade gliomas, seven metastases, five meningioma, and one cerebral abscess) using an axial spin-echo sequence with diffusion sensitizing gradients in the z direction and ECG triggering to minimize the influence of brain pulsations. They found that ADC in contrast-enhancing areas within cerebral metastases was significantly higher than ADC in contrast-enhancing areas in high grade gliomas. Furthermore, the ADC values in edema surrounding metastases were statistically significantly higher than the ADC values in edema around high grade gliomas. This finding may be helpful in distinguishing between these tumors.

The number of metastases in our study (two cases) is too small for statistical analysis of these findings. The ADC values of metastases were 0.82 and 1.24, whereas the enhancing part of the gliomas showed variation between 0.71 and 1.74. Considering the difficulty in distinguishing edema from tumor invasion in gliomas, this parameter was not calculated in our study. Furthermore, the ADC values for metastases and enhancing gliomas overlaps largely in the study presented by Krabbe et al (6) (1.2–2.73 and 0.72–2.61, respectively). Even if confirmed, this finding will have only relative value. The ADC values for meningioma reported by Krabbe et al (mean, 1.54) are similar to the ADC values of gliomas. This result is in agreement with our study.

Krabbe et al (6) also reported one case of abscess. The ADC value of the central part was 1.88×10^{-9} m^2/s. In our study, a central part of streptococcus abscess showed a striking hyperintensity on diffusion-weighted images with very low ADC values of 0.29. Similar behavior was observed in a case of multiple mucormycosis granulomas in a patient with AIDS (hyperintense on diffusion-weighted images with 0.39 ADC values). On the other hand, in a recent study of diffusion-weighted images in cases of acute stroke (1), one false positive finding (hyperintense on diffusion-weighted images) was a cerebral abscess.

All these results are in contradiction with the ADC value of abscess reported by Krabbe et al (6). A possible explanation for this discrepancy may be

a partial volume effect (only one section of 8 mm was used for diffusion-weighted imaging) or motion (examination time of 30 min with motion-sensitive spin-echo technique). The usefulness of diffusion-weighted MR imaging in the differential diagnosis between intracerebral necrotic tumors and cerebral abscesses was also recently confirmed by Desprechin at al (12).

In our study, two cases of lymphomas showed a good contrast with white matter on diffusion-weighted images and reduced ADC values (mean, 0.58). This may be useful in differentiation with gliomas and metastases, which showed higher ADC values (1.14 and 1.03, respectively).

To our knowledge, no data are available regarding the histologic analysis of tumors and diffusion-weighted imaging parameters. In our study, the contrast on diffusion-weighted images and ADC values of solid tumors correlated strongly with the volume of extracellular space. This finding supports the hypothesis that the low diffusion is mainly related to volume of extracellular space, as previously postulated in the mechanism of acute infarction (13, 14). In two cases of lymphoma (low ADC value) the volume of extracellular space was small; in all other tumors, including meningioma, the extracellular space was medium or large. This may explain why lymphomas were hyperintense on diffusion-weighted images although meningioma, metastases, and gliomas were not. There was not significant association between cellularity and ADC values. The lymphomas had high cellularity, but so did one metastases and one glioblastoma.

On the other hand, the diffusion-weighted imaging and ADC calculations were without significant relation with the malignancy of intra-axial tumors (including metastases and lymphomas). However, the number of cases per histology is small (only two grade II and two grade III astrocytomas), and a larger sample is needed.

Conclusion

Previous studies (4−6) reported variable results in the differentiation of tumors and edema by diffusion-weighted imaging. In our study, tumor delineation on diffusion-weighted images and ADC maps was generally poorer (except in two cases of lymphomas) than on T2-weighted spin-echo and/or contrast-enhanced T1-weighted spin-echo images. Therefore, the value of diffusion-weighted imaging and ADC maps in differentiation tumor/edema remains highly questionable.

In our study (limited number of patients), the lattice index maps showed a high contrast between high anisotropy white matter and tumor. However, the contrast between tumor, edema, and gray matter was much lower. The value of these more sophisticated calculated maps in differentiation of tumor/edema (diffusion lattice index, Eigen value sorted index map) needs further study.

Two cases of lymphomas also showed good contrast with white matter on diffusion-weighted images and reduced ADC values (mean, 0.58). This may be useful in differentiation with gliomas and metastases, which showed higher ADC values.

In our study, the contrast on diffusion-weighted images and the ADC values of solid tumors correlated strongly with the volume of extracellular space. This finding supports the hypothesis that the low diffusion is mainly related to the volume of extracellular space.

Acknowledgments

The authors express their gratitude to Filip De Ridder, Eddy Broodtaers, and Walter Rijsselaere for excellent technical support.

References

1. Lövblad KO, Laubach HJ, Baird AE, et al. **Clinical experience with diffusion-weighted MR in patients with acute stroke.** *AJNR Am J Neuroradiol* 1998;19:1061–1066
2. Benveniste H, Hedlund LW, Johnson GA. **Mechanism of detection of acute cerebral ischemia in rats by diffusion-weighted magnetic resonance microscopy.** *Stroke* 1992;23:746–754
3. Hossmann K-A, Fischer M, Bockhorst K, Hoehn-Berlage M. **NMR imaging of the apparent diffusion coefficient (ADC) for the evaluation of metabolic suppression and recovery after prolonged cerebral ischemia.** *J Cereb Blood Flow Metab* 1994; 14:723–731
4. Brunberg JA, Chenevert TL, McKeever PE, et al. **In vivo MR determination of water diffusion coefficients and diffusion anisotropy: correlation with structural alteration in gliomas of the cerebral hemispheres.** *AJNR Am J Neuroradiol* 1995;16: 361–371
5. Tien RD, Felsberg GJ, Friedman H, Brown M, MacFall J. **MR imaging of high-grade cerebral gliomas: value of diffusion-weighted echoplanar pulse sequences.** *AJR Am J Roentgenol* 1994;162:671–677
6. Krabbe K, Gideon P, Wagn P, Hansen U, Thomsen C, Madsen F. **MR diffusion imaging of human intracranial tumours.** *Neuroradiology* 1977;39:483–489
7. Pierpaoli C, Basser PJ. **Toward a quantitative assessment of diffusion anisotropy.** *Magn Reson Med* 1996;36:893–906
8. Tsuruda JS, Chew WM, Moseley ME, Norman D. **Diffusion-weighted MR imaging of the brain: value of differentiating between extraaxial cysts and epidermoid tumors.** *AJNR Am J Neuroradiol* 1990;11:925–934
9. Maeda M, Kawamura, Tamagawa Y, et al. **Intravoxel incoherent motion (IVIM) MRI in intracranial, extracranial tumors and cysts.** *J Comput Assist Tomogr* 1992;16:514–518
10. Tanner JE. **Intracellular diffusion of water.** *Arch Biochem Biophys* 1983;224:416–428
11. Chenevert TL, Brunberg JA, Pipe JG. **Anisotropic diffusion in human white matter: demonstration with MR techniques in vivo.** *Radiology* 1990;177:401–405
12. Desprechins B, Stadnik T, Koerts G, Shabana W, Breucq C, Osteaux M. **Use of Diffusion-Weighted MR Imaging in differential diagnosis between intracerebral necrotic tumors and cerebral abscesses.** *AJNR Am J Neuroradiol* 1999;20:1252–1257
13. Moseley ME, Cohen Y, Mintorovitch J, et al. **Early detection of regional cerebral ischemia in cats: comparison of diffusion and T2-weighted MRI and spectroscopy.** *Magn Reson Med* 1990;14: 31–39
14. Sevick RJ, Kucharczyk J, Mintorovitch J, Moseley ME, Deregin N, Norman D. **Diffusion-weighted MR imaging and T2-weighted MR imaging in acute cerebral ischemia: comparison and correlation with histopathology.** *Acta Neurochir Suppl (Wien)* 1992;51:210–212